



HAL
open science

Planktonic shift with dissolved organic matter properties: a functional perspective for sentinel lakes

Flavia Dory, Laurent Cavalli, Evelyne Franquet, Stéphane Mounier, Patrick Höhener, Benjamin Misson, Mathieu Martin, Quentin Arnault, Thierry Tatoni, Céline Bertrand

► To cite this version:

Flavia Dory, Laurent Cavalli, Evelyne Franquet, Stéphane Mounier, Patrick Höhener, et al.. Planktonic shift with dissolved organic matter properties: a functional perspective for sentinel lakes. *Journal of Ecology*, 2023, 111 (1), pp.45-61. 10.1111/1365-2745.14013 . hal-03816119

HAL Id: hal-03816119

<https://hal.science/hal-03816119>

Submitted on 15 Oct 2022

HAL is a multi-disciplinary open access archive for the deposit and dissemination of scientific research documents, whether they are published or not. The documents may come from teaching and research institutions in France or abroad, or from public or private research centers.

L'archive ouverte pluridisciplinaire **HAL**, est destinée au dépôt et à la diffusion de documents scientifiques de niveau recherche, publiés ou non, émanant des établissements d'enseignement et de recherche français ou étrangers, des laboratoires publics ou privés.

1 **Planktonic shift with dissolved organic matter**

2 **properties: a functional perspective for sentinel lakes**

3

4 Flavia Dory ^{a*}, Laurent Cavalli^a, Evelyne Franquet^a, Stéphane Mounier^b, Patrick Höhener^c,
5 Benjamin Misson^b, Mathieu Martin^a, Quentin Arnault^a, Thierry Tatoni^a, Céline Bertrand^a

6 ^a Aix Marseille Univ, Avignon Université, CNRS, IRD, IMBE, Marseille, France

7 ^b Univ Toulon, Aix Marseille University, CNRS/INSU, IRD, MIO UM 110, Mediterranean Institute of
8 Oceanography, CS 60584, 83041 – Toulon, France

9 ^c Aix Marseille University, CNRS, UMR 7376, Laboratory of Environmental Chemistry, Marseille,
10 France

11 **Contact Informations**

12 ***Corresponding author: Flavia Dory**, Aix Marseille Univ, Avignon Université, CNRS, IRD, IMBE,
13 Marseille, France

14 **E-mail address:** flavia.dory@imbe.fr ; **Phone:** 04 13 94 49 85; **Postal address:** 52 Av.
15 Escadrille Normandie Niemen, 13013 Marseille; **Orcid ID:** [https://orcid.org/0000-0002-5083-](https://orcid.org/0000-0002-5083-0737)
16 [0737](https://orcid.org/0000-0002-5083-0737)

17 laurent.cavalli@imbe.fr ; <https://orcid.org/0000-0001-9151-3247>

18 evelyne.franquet@imbe.fr ; <https://orcid.org/0000-0002-7779-772X>

19 stephane.mounier@mio.osupytheas.fr ; <https://orcid.org/0000-0002-9624-0230>

20 patrick.hohener@univ-amu.fr; <https://orcid.org/0000-0002-4453-566X>

21 benjamin.misson@mio.osupytheas.fr ; <https://orcid.org/0000-0002-4107-0916>

22 mathieu.martin4@orange.fr ; <https://orcid.org/0000-0002-8598-0102>

23 quentinarnault@hotmail.fr ; <https://orcid.org/0000-0001-6649-2018>

24 thierry.tatoni@imbe.fr ; <https://orcid.org/0000-0002-2557-4444>

25 celine.bertrand@imbe.fr ; <https://orcid.org/0000-0003-3085-3234>

26 **ABSTRACT**

27 1. Seasonal variations in mountain lakes regulate phytoplankton communities, which are thus
28 considered as useful indicators mirroring environmental conditions. Climate change is altering
29 both dissolved organic matter (DOM) properties and phytoplankton dynamics in sentinel
30 lakes. Here we examined the relationship between dissolved organic matter (DOM) and
31 planktonic communities to investigate how ecological functions in an oligotrophic lake
32 change over time. Physical, chemical, and biological data were analyzed during three pre-
33 defined periods running from complete ice-cover right to the end of the ice-free season to
34 assess the relationship between DOM, bacteria, and phytoplankton functional phenology.

35 2. The results showed that phytoplankton functional change occurred with dissolved organic
36 matter variation. Phytoplankton community was dominated by small size autotrophs and
37 mixotrophic flagellates during the *ice-influenced* period when DOM from sediment and
38 terrestrial origin dominated the DOM pool of the lake. Phytoplankton diversity and richness
39 increased during the post-snowmelt *overturn* period when terrestrial DOM dominated the
40 DOM pool of the lake. Finally, large siliceous autotrophs, competitive under small nitrogen
41 concentrations and high temperature, dominated almost exclusively the community during the
42 *late summer* period. Because increasing of phytoplankton biomass, phytoplankton-derived
43 DOM was dominant during the *late summer* period.

44 3. These phenological changes in phytoplankton community resulted in functional shifts at the
45 base of the food web: the nature of the relationship between phytoplankton and bacteria
46 progressively shifted, from strong top-down control exerted by phytoplankton over bacteria
47 toward predominantly bottom-up control at the end of the ice-free season.

48 4. *Synthesis*. Phenological functional shifts occur rapidly and are related to local processes,
49 like change in dissolved organic matter properties, nutrient limitation, temperature, and light

50 availability. Phytoplankton functional traits are useful indicators of whole ecosystem
51 ecological functioning.

52 **KEYWORDS**

53 Mountain lakes; Functional traits; Global change; Trophic interactions; Biogeochemical cycles

54 1. INTRODUCTION

55 In mountain lakes, phenological variations regulate phytoplankton communities, making them
56 useful indicators mirroring environmental conditions (Kuefner et al., 2021; Oleksy et al., 2020).
57 Phytoplankton communities during the ice-free season in high-altitude lakes have been widely
58 described. A large peak of phytoplankton biomass is typically observed in late summer (Pulido-
59 Villena et al., 2008; Tiberti et al., 2013), usually associated with shifts in community
60 composition and functional traits. Small unicellular flagellates have been observed in early
61 summer, followed by a shift toward less edible taxa in late summer, like large mucilaginous
62 colonies, flagellates (McKnight et al., 1990; Tiberti et al., 2013) or chlorophytes (Pulido-
63 Villena et al., 2008). However, this successional pattern is not always observed and depends on
64 the characteristics of the lakes (Jacquemin et al., 2019). Increasing data recorded on
65 phytoplankton community structure during winter in high-altitude lakes reveals patterns similar
66 to other seasonally ice-covered lakes (Özkundakci et al., 2016). Phytoplankton taxa show
67 functional traits that enable them to survive during winter under ice (Bertilsson et al., 2013),
68 like small size, motility, or mixotrophy (Rue et al., 2020). However, there are gaps in our
69 knowledge of how phytoplankton shifts occur between ice-covered and ice-free seasons, and
70 how functional shifts may affect whole lake ecosystem functioning.

71 Dissolved organic matter (DOM) is a very good sensor for mountain lake structure and function
72 (Aiken, 2014). High-altitude lakes traditionally exhibit an autochthonous DOM fluorescence
73 signature (Bastidas Navarro et al., 2014; Sommaruga & Augustin, 2006). Nevertheless, DOM
74 origin can vary at short-term, seasonal, and interannual time scales. For example, allochthonous
75 DOM can be transferred to lakes during snowmelt and extreme rainfall events at high altitude
76 (Perga et al., 2018; Sadro et al., 2011). An advancing treeline due to temperature increase, as
77 well as more frequent extreme precipitation events, may enhance allochthonous inputs in
78 mountain lakes and their connectivity with their surrounding catchments (Harsch et al., 2009).

79 DOM dynamics strongly affect internal lake processes through direct and indirect
80 transformations at the base of the food web (Creed et al., 2018). Seasonal variations in DOM
81 origin and nutrient limitation patterns in high-altitude lakes should lead to temporal variations
82 in microbial interactions (Jacquemin et al., 2018). Depending on the nutrient limitation, increase
83 of allochthonous C has been shown to reduce bacterial reliance on phytoplankton-produced
84 carbon (Jansson et al., 2000), stimulate bacterial biomass, and increase predation over bacteria
85 by mixotrophs (Bergström, 2009). Experimental DOC and nutrient additions have induced
86 different interaction between bacterioplankton and phytoplankton in winter, early summer, or
87 in late summer in a high-altitude lake (Dory et al., 2021; Dory et al., unpublished results). Thus,
88 a clearer picture is needed of how the phytoplankton-bacterioplankton relationship varies from
89 the ice-covered to the ice-free season according to DOM dynamics in high-altitude lakes.

90 High-altitude lakes have been identified as sentinels of global change (Moser et al., 2019).
91 However, their value as sentinels is highly dependent on how well we understand their internal
92 processes, determined to a large extent by climate seasonality (Catalan, Ventura, et al., 2002).
93 The functioning of high-altitude lakes is traditionally divided into ice-covered and ice-free
94 periods, and most studies focus on one period. Based on various lake indicators, however, some
95 studies track temporal changes on a finer scale to further describe internal lake processes. By
96 analyzing changes in microbial assemblages, Felip et al. (2002) discriminated between three
97 periods of winter cover in an alpine high mountain lake. Ecosystem metabolism (Sadro et al.,
98 2011) and DOM dynamics (Olson et al., 2021) allowed to highlight a snowmelt influence until
99 late July or after the beginning of August. Tiberti et al. (2013) observed a late summer peak of
100 phytoplankton biomass in October, slightly behind the physico-chemical variations.

101 We considered three periods ranging from complete ice-cover to the end of the ice-free season
102 in an alpine lake: (i) the ice-influenced period; (ii) the overturn period; (iii) the late summer
103 period. The temporal dynamics of dissolved organic matter (DOM) and planktonic

104 communities over these three periods were examined to better understand how lake ecological
105 functions change over time. We hypothesized that the signature of DOM would be less
106 influenced by allochthonous inputs and phytoplankton production during the ice-influenced
107 period, mainly determined by allochthonous inputs during the overturn period, and mainly
108 determined by primary production during the late summer period. We also anticipated
109 phytoplankton functional changes according to environmental variations, with more winter-
110 adapted traits and mixotrophic taxa during the ice-influenced period and more autotrophy
111 during the ice-free season. Finally, we expected functional shifts at the base of the food web
112 with a modified balance between heterotrophy and autotrophy, linked to the temporal dynamics
113 of DOM, bacterioplankton, and phytoplankton communities.

114 2. MATERIALS AND METHODS

115 2.1. Lake area, sampling, and definition of time periods

116 Samplings were performed in the oligotrophic high-altitude Lake Cordes (Dory et al., 2021a).
117 The lake was sampled 11 times between February 2020 and July 2021, divided into three
118 periods. The lake was sampled four times during the ice-influenced period (IIP, from February
119 to mid-June), four times during the overturn period (OP, from mid-June to late July), and three
120 times during the late summer period (LSP, from August to October) (**Table A1**). On every date,
121 samples were collected from the deepest area of the lake. Water was sampled using a Niskin
122 Bottle 1 m above the bottom and 1 m below the surface. All the samples were realized in
123 triplicate and then fixed and stored in the field in containers appropriate to the analyses to be
124 performed in the laboratory. Abiotic parameters of temperature, dissolved oxygen, and turbidity
125 were monitored using an Exo2 multiparameter probe (YSI, United States) placed 1 m above the
126 lake bottom.

127 2.2. Biotic and abiotic parameters

128 2.2.1. Environmental and climate parameters

129 Water properties of the lake (temperature, dissolved oxygen, and turbidity) were averaged from
130 continuous data measured by the multiparameter probe. Data were obtained every hour and a
131 daily average was calculated for each sampling day. Daily precipitations were taken from a
132 weather station located about 14 km from the lake, and data were collected from the alpine
133 meteorological observation network (ROMMA, <http://romma.org/>). Average precipitations
134 were calculated from the 10 days preceding the sampling date.

135 2.2.2. Nutrients (C, N, P, Si)

136 Water samples of 1L for nutrient analysis were filtered through precombusted (4h, 450°C) GF/F
137 glass filters (Whatman GF/F, 25 mm, 0.7 µm). A first fraction of the filtered water was stored
138 in 24 ml precombusted (4h, 450°C) glass tubes (Wheaton equipped with Teflon/silicon septa)
139 and preserved with 25 µL of Sodium Azide solution (1 M NaN₃) at 4°C for dissolved organic
140 carbon (DOC) analysis and dissolved organic matter (DOM) fluorescence measurements. DOC
141 concentrations were measured using a TOC-VCSH analyzer (Shimadzu, TOC-V). A second
142 filtered fraction was stored in 150 ml HDPE bottles and frozen (-18°C) for analysis of dissolved
143 inorganic nitrogen (DIN = NH₄⁺ + NO₂⁻ + NO₃⁻), soluble reactive phosphorus (SRP = PO₄³⁻),
144 and Silica (Si). DIN, SRP, and Si were measured by ion chromatography (Metrohm, 930
145 Compact IC Flex).

146 2.2.3. C:N ratio and C isotopic analyses

147 C:N ratios and analyses of carbon stable isotope (δ¹³C) in particulate organic matter (POM)
148 were performed from June 2020 to September 2020 and in May 2021. Water samples were
149 filtered (0.7 – 20 µm) to concentrate the finest fraction of the seston, consisting mainly of
150 phytoplankton. Filters were then dried at 60°C and decarbonated by acid-fuming (HCl 37%)
151 for analysis. Samples were ground (RETSCH Mixer Mill MM 400), then between 0.2 and 0.6
152 mg of homogeneous samples were weighed into tin capsules (three capsules per sample). C and

153 N abundances and $\delta^{13}\text{C}$ ratios were analyzed using an Elemental analyzer (EA, Flash HT plus
154 - Thermo Scientific) equipped with an autosampler configured with a combustion reactor for
155 carbon and nitrogen analyses. The elemental analyzer is connected to an isotope ratio mass
156 spectrometer (IrMS "Delta V Advantage", Thermo Scientific). Organic carbon and total
157 nitrogen contents were determined from the signal of the TCD detector in the Elemental
158 Analyzer. The C and N values obtained were used to calculate the C:N ratio of the suspended
159 particulate organic matter (POM) in the water sample. C:N values were measured from June
160 2020 to September 2020 and in March and May 2021. $\delta^{13}\text{C}$ (‰) values were expressed relative
161 to the international reference (Vienna-Pee Dee Belemnite, V-PDB) using the equation 1 and
162 0.011237 for R_{standard} :

$$163 \quad \delta^{13}\text{C} (\text{‰}) = \left(\frac{R_{\text{sample}}}{R_{\text{standard}}} - 1 \right) \times 1000 \quad (1)$$

164 The $\delta^{13}\text{C}$ determination was calibrated by a two-point method using the international standard
165 NBS-22 and a laboratory standard for urea.

166 2.2.4. DOM extractions

167 Leachates of four sources of organic matter were used to characterize the fluorescence signature
168 of dissolved organic matter in Lake Cordes. The soil and alpine grass were collected randomly
169 in the watershed on each sample date. When present, common macrophyte species were
170 collected and cleaned by repeated rinsing in distilled water. Sediment samples were taken at
171 each sample date with an Ekman grab. All samples were freeze-dried, ground, and sifted
172 through a 2 mm mesh sieve. The samples were extracted with Milli-Q water (solid to water
173 ratio, w/v = 0.1), the suspensions were placed at 4°C and stirred manually within 24 h. The
174 suspensions were then centrifuged (10 000 rpm, 20 min), filtered (pre-combusted GF/F), and
175 subsequently stored at 4 °C until analysis.

176 2.2.5. Absorbance and fluorescence measurements

177 Leachates and natural water samples were analyzed for UV-vis spectra using a
178 Spectrophotometer V-550 (Jasco) with 10-cm Suprasil quartz cells. Water was scanned between
179 230 and 800 nm using a 1000 nm.min⁻¹ scan rate and 0.5 nm resolution. Milli-Q water was used
180 as a blank and subtracted from each sample. Fluorescence measurements were performed using
181 a spectrofluorometer (F4500, Hitachi, Santa Clara, California, USA) equipped with a 450W
182 xenon lamp. The spectra were acquired in the scan ranges of 200–600 nm for emission and
183 excitation, with both slits fixed at 5 nm using 1 cm quartz Suprasil cell. The scan speed was set
184 at 2400 nm.min⁻¹, and the detector voltage was 700 V. Fluorescence intensity was normalized
185 to Raman units (R.U.) using the daily-measured Raman peak of Mili-Q water ($\lambda_{ex} = 350$ nm,
186 $\lambda_{em} = 371$ – 428 nm). The collected EEMs were analyzed using parallel factor analysis
187 (PARAFAC), to identify the different components of the FDOM pool. PARAFAC was
188 conducted on the EEM dataset using Progmee software (Redon, 2018) in Matlab language.
189 PARAFAC was applied to the complete dataset containing all the EEMs (leachates and water
190 samples of DOM). Three fluorescence indexes were used to characterize the FDOM: the
191 humification index (HIX), the freshness index (BIX), and the fluorescence index (FI). The HIX
192 is calculated as the sum of emissions ranging between 435 and 480 nm, divided by the sum of
193 emissions ranging between 300 and 345 nm, at an excitation intensity of 255 nm, corrected
194 according to the procedure of Ohno (2002). The BIX is the ratio of emission intensity at 380
195 nm divided by maximum emission intensity between 420 and 435 nm, at an excitation intensity
196 of 310 nm. The BIX value reflects the contribution of recent (autochthonous) organic matter to
197 the organic matter pool. Low ratios are interpreted as a low contribution of autochthonous
198 organic matter, while high ratios correlate with a strong contribution of recent autochthonous
199 organic matter (Gabor et al., 2014). Finally, the FI is the ratio of emission intensity between
200 470 and 520 nm, at an excitation intensity of 370 nm (Cory & McKnight, 2005). The

201 fluorescence index indicates whether the DOM precursor material is more microbial in nature
202 (FI ~ 1.8) or is of terrestrial origin (FI ~ 1.2).

203 2.2.6. Phytoplankton analyses

204 Phytoplankton samples were fixed with a formaldehyde solution (5%) and stored in 250 ml
205 HDPE bottles. Phytoplankton counts were performed according to the Utermöhl (1958)
206 method, at 40-fold magnification under an inverted microscope (Olympus IX 70).
207 Phytoplankton samples were identified at genus level and species level when possible, using
208 appropriate taxonomic guides. Phytoplankton biovolume was estimated by shape assimilation
209 to known geometric forms and direct measurement of the main cell dimensions. Then the
210 biovolume was converted into biomass using the particular carbon content defined for each
211 class by Wetzel & Likens (2000). Phytoplankton taxa were classified in four groups: (i)
212 taxonomic groups (**TAX**) based on their main phylogenetic affiliations; (ii) protist functional
213 groups (**PFG**) based on their nutrient acquisition, *i.e.* photoautotrophs lacking phagotrophy
214 capacity (**PA**) and constitutive mixotrophs (**CM**) (Mitra et al., 2016); (iii) morphology-based
215 functional groups (**MBFG**) based on their morphological traits (Kruk et al., 2010); and (iv)
216 functional groups (**FG**) based on their morphology and physiology and on the similarity of their
217 ecological characteristics (Padisák et al., 2009; Reynolds et al., 2002). Phytoplankton diversity
218 was characterized according to two indexes: the Species richness index (S) measures the total
219 number of phytoplankton species in each sample, and the Shannon index (H') takes into account
220 both the richness and evenness of the species present in each sample. Ciliate abundances were
221 also estimated via the Utermöhl method.

222 2.2.7. Picoplankton

223 Water samples (1.5 ml) were filtered (20 µm) and analyzed for picoplankton analyses by flow
224 cytometry. Samples were fixed with glutaraldehyde (0.25% final concentration) and stored at

225 –80°C until flow cytometry analysis. Picoplankton was characterized and enumerated using an
226 Accuri C6 flow cytometer equipped with a blue laser (488 nm) and using BD Accuri CFlow
227 Plus Analysis software (BD-Biosciences). Non-fluorescent polystyrene microspheres (Flow
228 Cytometry Size Calibration Kit, Thermo Fisher Scientific) were used as a size standard. For
229 picocyanobacteria, 500 µl of sample were run at fast speed (66 µl/min). Picocyanobacteria
230 (PCY) were identified by their small size (FSC < 2 µm), low complexity (SSC), and
231 fluorescence (emissions in the orange and red wavelength ranges, respectively 585 ± 20 and
232 >670 nm). Flow cytometer analysis distinguished between two groups of picocyanobacteria:
233 cells with high orange fluorescence were classified as phycoerythrin-rich picocyanobacteria
234 (PE-Pcy); cells with low orange and high dark red fluorescence were classified as
235 phycocyanine-rich picocyanobacteria (PC-Pcy). For heterotrophic prokaryotes (HP), samples
236 were stained with 1:10,000 (vol/vol) SYBR® Green II and incubated 20 min in darkness. 50 µl
237 of stained samples were run at medium speed (35 µl/min). HP were identified by their small
238 size (low FSC), low complexity (low SSC), high green fluorescence (530 ± 15 nm), and lack
239 of red (> 670 nm) fluorescence. Picoplankton data were acquired and analyzed using BD Accuri
240 CFlow Plus Analysis software (BD-Biosciences). Abundances were transformed into carbon
241 content based on the literature. Cell abundance (cells/ml) of HP was converted to biomass (µg
242 C/L) using 20 fg C/cell as constant conversion factor (Linacre et al., 2015). A conversion factor
243 of 112 fg C/cell was used for picocyanobacteria (Linacre et al., 2015).

244 **2.3. Statistical analyses**

245 One-way ANOVA tests followed by pairwise comparisons were used to test the effect of period
246 on the various abiotic and biological variables measured, and to test differences in fluorescence
247 characteristics between the four leachates of organic matter sources. Non-metric
248 multidimensional scaling (NMDS) analysis was performed on a Bray-Curtis distance matrix to
249 visualize the differences in taxonomic structure of the phytoplankton community between

250 periods. To test the hypothesis that the taxonomic distribution of the phytoplankton community
251 was structured by period, a multivariate permutation analysis of variance (permanova) was used
252 with 999 permutations ($p = 0.05$) with the adonis function in R. A multivariate homogeneity
253 analysis of group dispersion (β diversity) was used to assess the homogeneity of phytoplankton
254 assemblages within a group of samples (betadisper function). Canonical Correspondence
255 Analysis (CCA) was performed to explore the distribution of the different phytoplankton
256 taxonomical groups in relation to the measured explanatory variables. The significance of the
257 phytoplankton composition variance explained by the selected abiotic variables was assessed
258 by permutation tests. All analyses were performed with R 3.6.3 (R Core Team, 2018).

259

260 3. RESULTS

261 **3.1. Abiotic and climate parameters**

262 The ice-influenced period (IIP) was characterized by significantly lower concentrations of
263 dissolved oxygen, temperature, and precipitations (**Figure 1**). Turbidity was significantly
264 greater during this period, but highly variable. SRP concentrations were low during the ice-
265 influenced period, whereas silica and DIN concentrations were high and highly variable.
266 Ammonium was the dominant N source of the DIN pool during IIP ($73 \pm 13\%$, data not
267 showed). Particulate organic matter (POM) showed the most negative $\delta^{13}\text{C}$ values and low C:N
268 values.

269 During the overturn period (OP), many abiotic parameters significantly increased, such as
270 dissolved oxygen, temperature, precipitations, and SRP concentrations. The $\delta^{13}\text{C}$ values and
271 C:N of POM also significantly increased during OP, whereas turbidity and silica concentrations
272 were significantly lower than during IIP. While there was no significant change in DIN
273 concentrations, they were less variable. Nevertheless, within the DIN pool, nitrite became
274 dominant over ammonium during OP ($88 \pm 7\%$, data not showed).

275 The late summer period (LSP) did not significantly differ from OP for any abiotic parameters
276 except $\delta^{13}\text{C}_{\text{POM}}$ which showed significantly higher values, and C:N of POM. However, LSP
277 was significantly different from IIP for all parameters except SRP concentrations and C:N of
278 POM. This period was characterized by higher variability in temperature and precipitations.

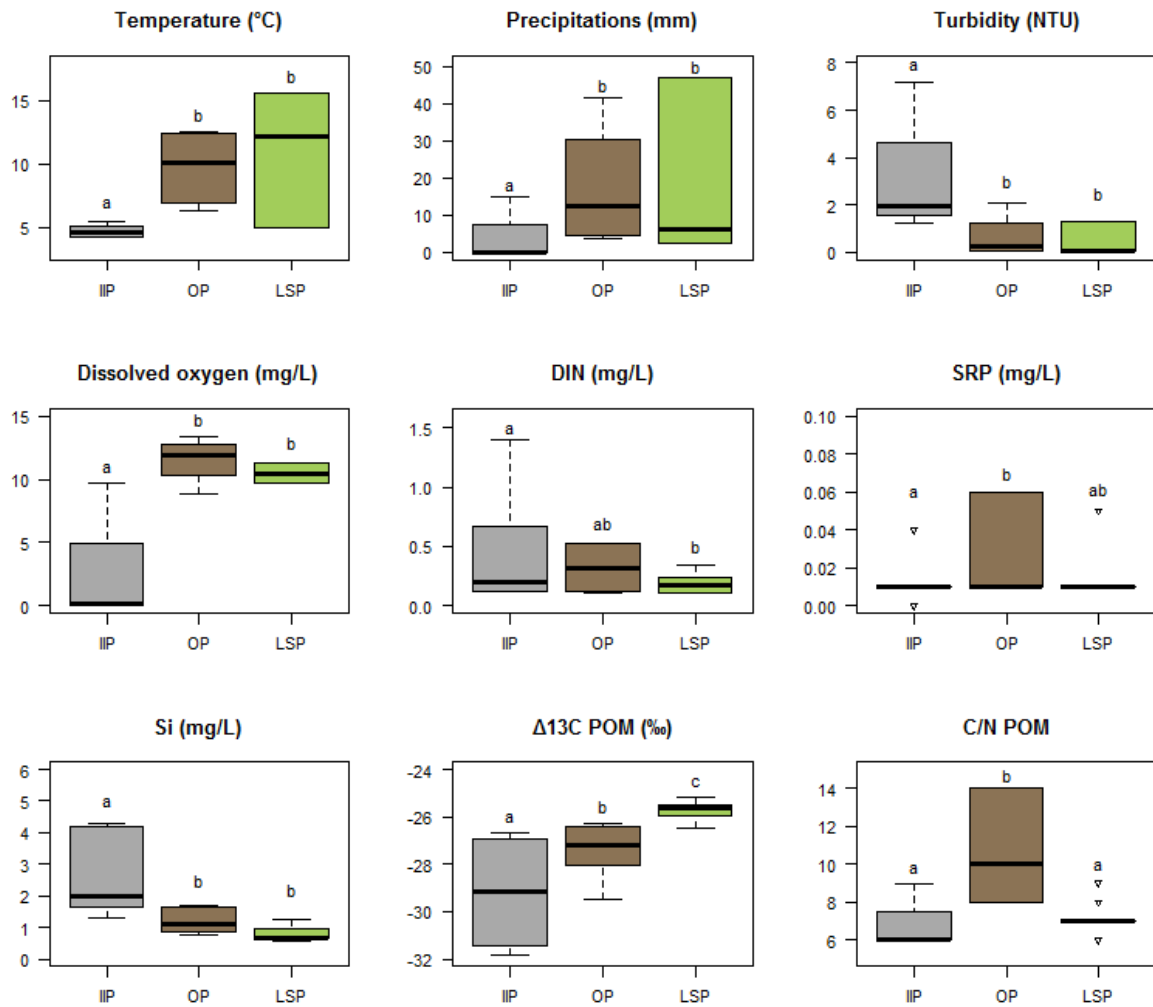


Figure 1: Abiotic and climate parameters measured in the three defined functional periods in Lake Cordes. DIN: dissolved inorganic nitrogen; SRP: soluble reactive phosphorus; Si: silica; POM: particulate organic matter.

280 **3.2. Characterization and dynamics of DOM**

281 3.2.1. *Identification of the components by PARAFAC modeling*

282 PARAFAC analysis of the EEM spectra of leachates and water samples identified four
283 fluorescent components (C1, C2, C3, and C4) (**Figure 2**). C1 and C4 are known to be non-
284 humic compounds: C1 (Ex/Em = 300/350 nm) is linked to soluble microbial byproduct-like
285 material (Chen et al., 2003), while C4 (Ex/Em = 230-270/350 nm) is often linked to simple
286 aromatic proteins such as tyrosine. Conversely, C2 and C3 are considered humic-like
287 compounds: C2 (Ex/Em = 250-310/450 nm) is referred to as a combined component constituted
288 by humic acid-like and fulvic acid-like materials. C3 (Ex/Em = 270(360)/460 nm) has been
289 associated with humic acid-like organics (Murphy et al., 2008).

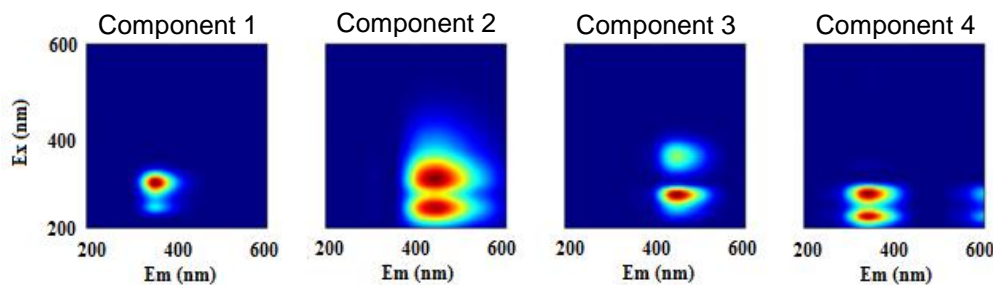


Figure 2: PARAFAC model output showing fluorescence signatures of the four fluorescent components identified in the 4 leachates and in water samples.

290

291 3.2.2. *Fluorescence signature of the sources of DOM*

292 Regarding the “internal” sources, the macrophytes leachate fluorescence response was mainly
293 dominated by C4, while the sediment leachate fluorescence response was mainly dominated by
294 C3 (**Figure 3A**). Regarding the “external” sources, the soil and the grass leachate fluorescence
295 were mainly dominated by C2 and C4.

296 HIX values varied significantly between sources (Anova, $F = 14.9$, $p\text{-value} < 0.001$), with a
 297 greater predominance of humic compounds in the sediment and soil leachates than in the
 298 macrophytes and grass leachates (**Figure 3B**). BIX values were significantly higher in the two
 299 internal sources than in the two external sources (Anova, $F = 17.9$, $p\text{-value} < 0.001$). Finally, FI
 300 values were significantly higher in the sediment leachate ($FI = 1.89 \pm 0.2$) than in the other
 301 sources, and were lowest in the soil leachate ($FI = 1.16 \pm 0.04$) (Anova, $F = 42.6$, $p\text{-}$
 302 $\text{value} < 0.001$) (**Figure 3C**).

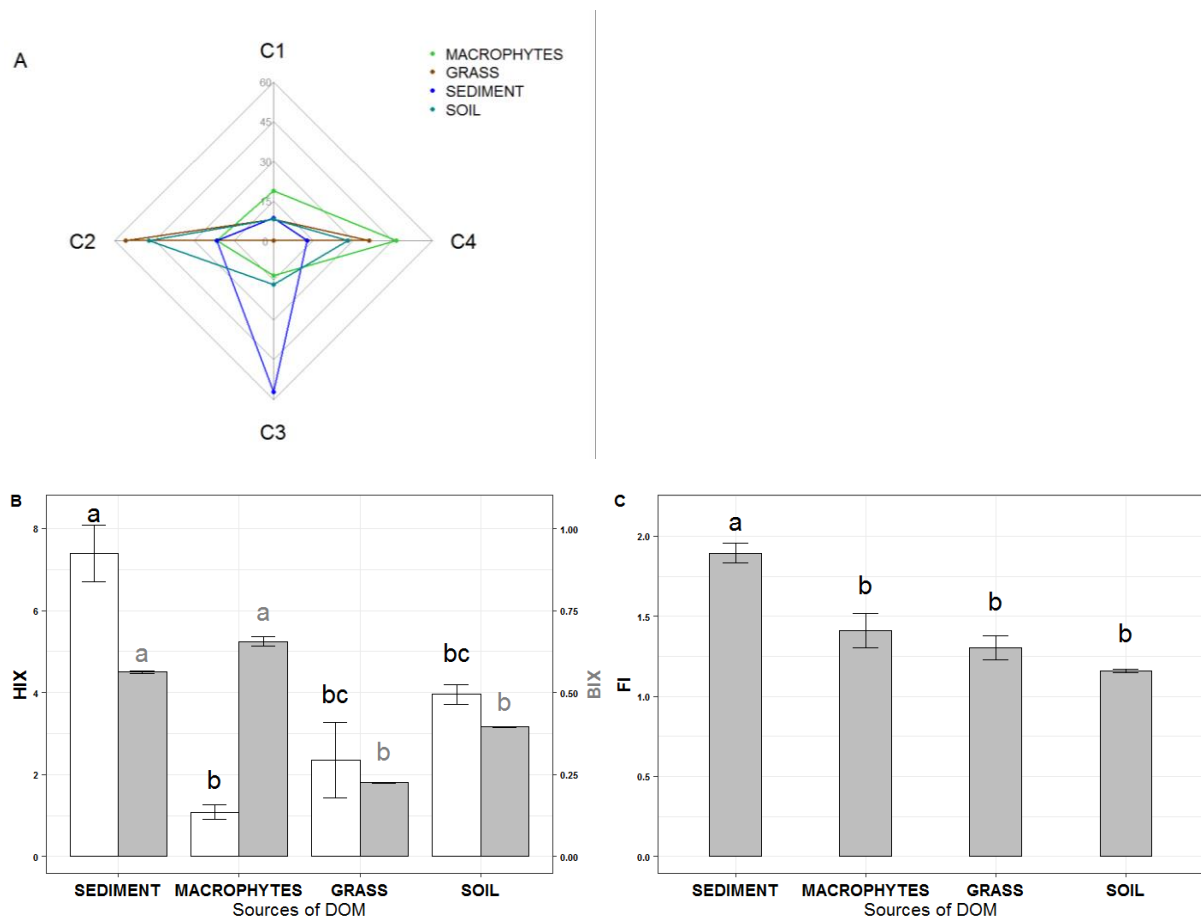


Figure 3: (A) Relative contribution of the four components for the four leachates of dissolved organic matter (DOM) sources; (B) Humification index (HIX) in white and freshness index (BIX) in grey of the four leachates of DOM sources; (C) Fluorescence index of the four leachates of DOM sources.

303

304

305 3.2.3. *Dynamic signature of lake DOM*

306 During the ice-influenced period (IIP), significantly higher values for FI, HIX, and the
307 proportion of C3 were observed than during the two other periods (**Figure 4**). The proportion
308 of C2 was also high. This period was also characterized by moderate but variable DOC
309 concentrations and a moderate proportion of C4. The overturn period (OP) was characterized
310 by significantly lower HIX and FI values than during IIP, while BIX values did not differ
311 significantly, remaining low. Measured DOC concentrations were low. OP was characterized
312 by a high proportion of C2 and C4 and a low proportion of C1. Finally, during the late summer
313 period (LSP), BIX values were significantly higher than during the two other periods,
314 associated with low but variable values of FI and HIX. DOC concentrations and C1 proportion
315 were higher in LSP, while the proportions of C2, C3 and C4 were low. It is noteworthy that,
316 the late summer period was characterized by higher variability in all parameters except DOC.

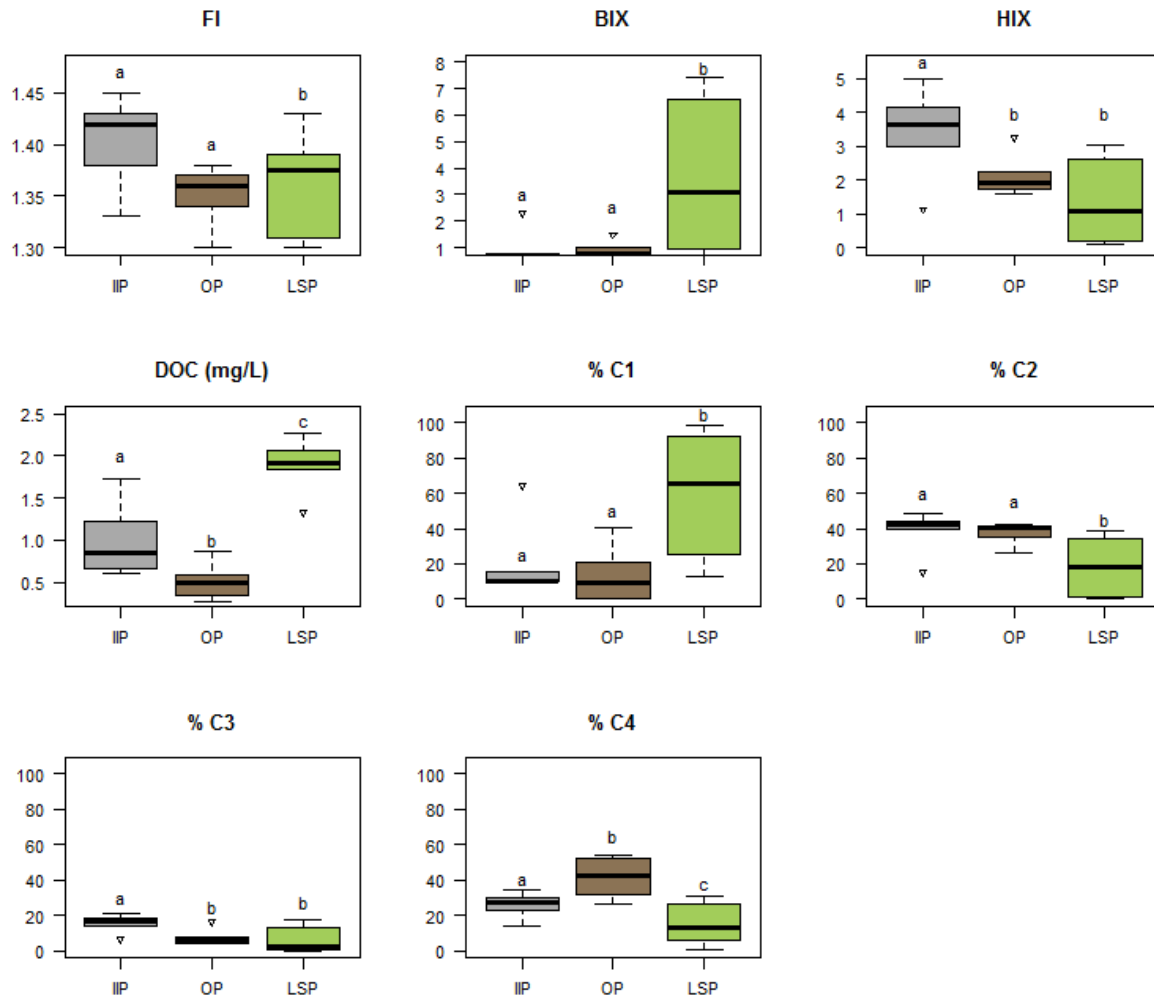


Figure 4: DOM characteristics measured in the three defined periods in Lake Cordes. DOC: dissolved organic carbon.

317

318 3.3. Planktonic community dynamics

319 Phytoplankton biomass was low during the ice-influenced period (IIP) and the overturn period
 320 (OP), increasing significantly during the late summer period (LSP) (**Figure 5**). While specific
 321 richness increased progressively from IIP to LSP, the Shannon diversity index was significantly
 322 higher in OP than during the two other periods. HP biomass increased progressively over the
 323 three periods. Ciliate abundance was low during IIP and OP, then significantly increased during
 324 LSP.

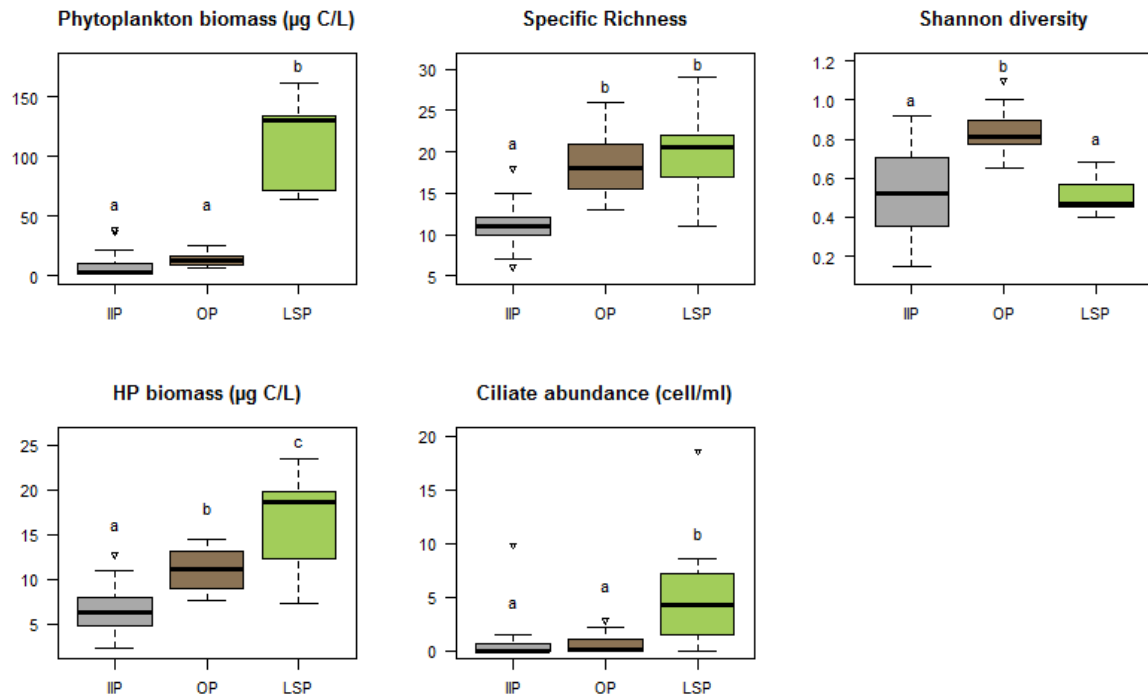


Figure 5: Biological parameters measured in the three defined periods in Lake Cordes. HP: heterotrophic prokaryotes.

325

326 Concerning taxonomical and functional changes in phytoplankton assemblages, a significant
 327 shift in phytoplankton community structure was observed over the three periods (**Figure A1**,
 328 Adonis, $F = 29.362$, $r^2 = 0.57$, $p\text{-value} < 0.001$). Cyanobacteria dominated the other
 329 phytoplankton groups during IIP (**Figure 6**), which also showed a high proportion of
 330 cryptophytes, dinoflagellates, and phycoerythrin-rich picocyanobacteria (PE_Pcy). A relatively
 331 high proportion of constitutive mixotrophs was found during IIP (45%), as well as MBFG
 332 groups I (small cells with high surface/volume ratio) and V (flagellates of medium to large size)
 333 and FG groups K (shallow, nutrient-rich water column) and Y (small, enriched lakes, lentic
 334 ecosystems with low grazer pressure). OP was characterized by an increased proportion of
 335 diatoms (51%), which became dominant over the other phytoplankton groups. Dominance by
 336 the PE_rich PCy was replaced by that of the phycocyanin-rich picocyanobacteria (PC_Pcy).
 337 The relative proportion of mixotrophs remained high (45%). Among the mixotrophic taxa,

338 while the proportion of dinoflagellates remained the same as during IIP, an increase in the
 339 proportion of chrysophytes was observed together with a decrease in the proportion of
 340 cryptophytes. The proportion of MBFG groups II (small siliceous flagellates) and VI (non-
 341 flagellated with siliceous exoskeletons) increased, as did FG groups A (clear, deep, often well-
 342 mixed lakes), Lo (all lentic ecosystems), and MP (all types of lakes, or frequently stirred up,
 343 inorganically turbid shallow lakes). During LSP, the phytoplankton assemblage was mainly
 344 composed of diatoms (89%), corresponding to the high proportion of MBFG group VI and FG
 345 group MP. PC_Pcy dominated the pool of picocyanobacteria in LSP.

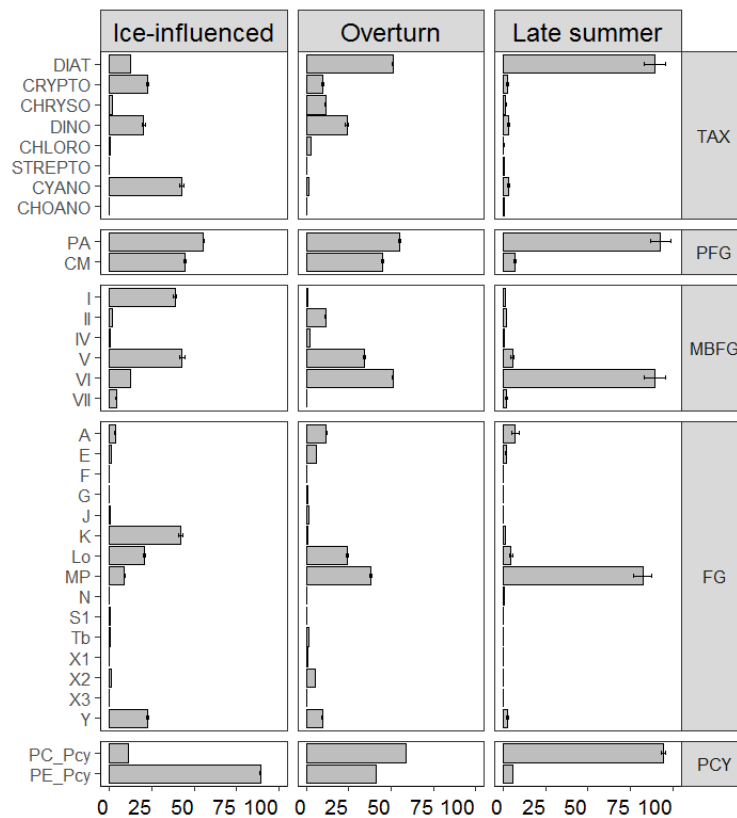


Figure 6: Phytoplankton composition in each period (error bars correspond to standard error). DIAT = diatoms; CRYPTO = cryptophytes; CHRYSO = chrysophytes; DINO = dinoflagellates; CHLORO = chlorophytes; STREPTO = Streptophytes; CYANO = cyanobacteria; CHOANO = choanoflagellates; PA = photoautotrophic phytoplankton; CM = constitutive mixotrophs; PE_Pcy = phycoerythrin-rich picocyanobacteria; PC_Pcy = phycocyanin-rich picocyanobacteria.

347 **3.4. Links between microbial plankton and dissolved organic matter**

348 CCA was conducted with phytoplankton taxonomical groups as response variables and abiotic
349 parameters, and HP biomass and ciliate abundance as explanatory variables (**Figure 7**). The
350 constrained variables explained 87% of inertia, and the eigenvalues for the first and second
351 sorting axes were 0.178 and 0.075, respectively. Dissolved oxygen, HP biomass, FI,
352 temperature, and turbidity showed far higher correlation coefficients with the first axis (-0.87,
353 -0.63, 0.58, -0.56, and 0.55, respectively), suggesting that these explanatory variables played a
354 predominant role in affecting the taxonomic composition of the phytoplankton community.
355 PE_PCY, cyanobacteria and cryptophytes were associated with higher silica concentrations,
356 higher proportions of C3, higher HIX values, higher turbidity, but lower dissolved oxygen
357 concentrations during the ice-influenced period. The second axis discriminated between
358 overturn and late summer periods, and DOC concentrations and C1 proportions were
359 particularly high and positively correlated with the late summer period. Both OP and LSP were
360 characterized by an increase in diatoms, while chrysophytes and chlorophytes were particularly
361 prevalent during OP.

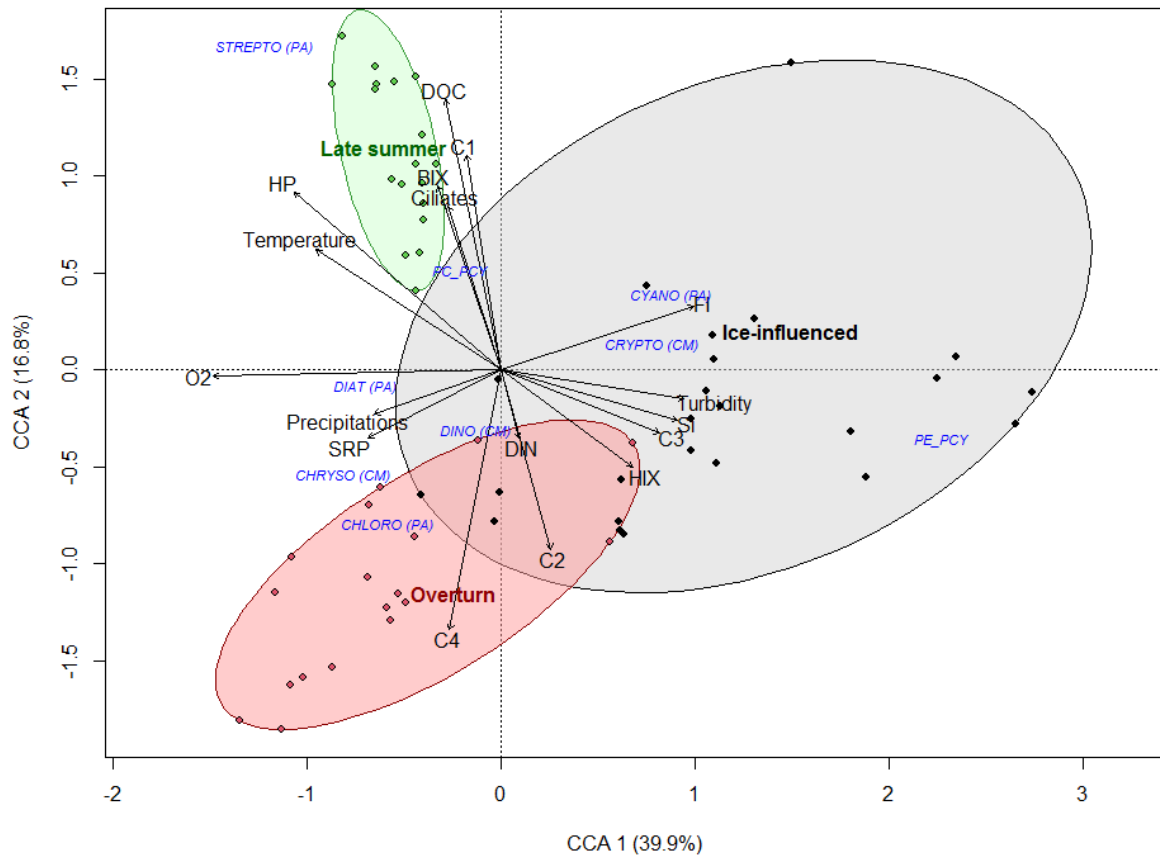


Figure 7: CCA performed on the taxonomic phytoplankton groups (and their corresponding PFG classification) and picophytoplankton groups (PCY) in relation to explanatory variables. DOC: dissolved organic carbon; HP: heterotrophic prokaryotes; O₂: dissolved oxygen; SRP: soluble reactive phosphorus; DIN: dissolved inorganic nitrogen; Si: silica; CYANO: cyanobacteria; CRYPTO: cryptophytes; DINO: dinoflagellates; CHLORO: chlorophytes; CHRYSO: chrysophytes; DIAT: diatoms; STREPTO: Streptophytes; PC_PCY: phycocyanin-rich picocyanobacteria; PE_PCY: phycoerythrin-rich picocyanobacteria.

362

363

364 4. DISCUSSION

365 4.1. Variation in DOM origin

366 We characterized the fluorescence signature of four sources of DOM to better understand DOM
367 dynamics in Lake Cordes. All the DOM sources exhibited a specific fluorescent signature and,
368 interestingly, none of the four sources of DOM exhibited a C1-dominated signature. Our
369 findings demonstrate that the origin of DOM varied greatly over the three periods in Lake
370 Cordes (**Figure 8**). The ice-influenced period exhibited the highest FI values (1.41). In previous
371 studies in high-altitude lakes, FI values of 1.44 were considered to be low and to reflect a more
372 allochthonous DOM pool (Miller et al., 2009; Rose et al., 2015). However, the associated high
373 HIX values (3.43) and low BIX values (0.96) suggest a refractory and humic DOM linked to a
374 microbial precursor material (Du et al., 2016; Ohno, 2002). The low C:N values observed for
375 POM confirm a more autochthonous origin for DOM during the ice-influenced period.
376 Moreover, the ice-influenced period showed the highest proportion of C3, indicating a higher
377 contribution of the sediment to the DOM pool than during the two other periods. However,
378 allochthonous inputs of DOM also occurred during the ice-influenced period, as suggested by
379 the highly variable C:N values of POM and the relatively high proportion of C2 and C4. Similar
380 results were previously observed during winter in a subarctic clear-water lake (Karlsson et al.,
381 2008), where sediment organic carbon was the dominant carbon source for respiration under
382 the ice, but both allochthonous and autochthonous carbon contributed to DIC accumulation in
383 the lake. In our study, such allochthonous inputs likely started at the end of the ice-influenced
384 period, when the snowmelt occurred.

385 During the overturn period, DOM showed the lowest FI (1.35) and BIX (0.90) values and
386 moderate HIX (2.12) values, suggesting a more refractory, terrestrial origin for DOM than
387 during the ice-influenced period. The C:N values of POM and the contribution of C2 and C4 to
388 FDOM were highest during the overturn period, confirming the hypothesis of a higher

389 contribution of the DOM pool originating from the catchment area. Despite the predominant
390 soil signature of the DOM during the overturn period, however, low DOC concentrations were
391 measured in the water column. It is therefore possible that DOC inflows occurred earlier, at the
392 end of the ice-influenced period when the snow and ice started to melt. Indeed, DOC can rapidly
393 be degraded after allochthonous DOM inputs (Catalán et al., 2013). These low DOC
394 concentrations may also be explained by low DOC content in the allochthonous DOM
395 transferred to the lakes (Queimaliños et al., 2019) and a strong dilution effect during snowmelt
396 or rain events involving shorter water residence (Anderson & Stedmon, 2007).

397 During the late summer period of our study, C1 was predominant in DOM. This component
398 was not associated with a specific fluorescence signature of the four leachate sources of DOM
399 but was associated with higher DOC concentrations and higher phytoplankton biomass.
400 Moreover, DOM showed low but highly variable HIX values (1.35) and high BIX values (3.65),
401 suggesting a high contribution of fresh, autochthonous DOM. However, FI values were also
402 low (1.36) thus not indicative of organic material derived from algae and bacteria. Like the
403 other fluorescence indexes, FI was highly variable during the late summer period, and
404 particularly low at the October sampling. Heavy precipitations occurred during October,
405 possibly driving allochthonous inputs into the lake and modifying the autochthonous signature
406 of the DOM. Thus, despite a variable signature, our results suggest that DOM mainly originated
407 from phytoplankton development in the water column during the late summer period. These
408 findings are consistent with other studies in mountain lakes showing a higher contribution of
409 phytoplankton to the DOM pool at the end of the ice-free period (Sadro & Melack, 2012;
410 Sommaruga & Augustin, 2006).

411 **4.2. Phytoplankton functional changes**

412 Our results highlight the high sensitivity to environmental variations of phytoplankton
413 assemblages, whose structure and composition changed according to shifts in lake functioning

414 **(Figure 8)**. During the ice-influenced period, phytoplankton biomass was low and the
415 assemblage was dominated by small autotrophs with a high surface/volume ratio, and by large
416 mixotrophic flagellates. Mixotrophs represented 45% of the phytoplankton assemblage, mainly
417 cryptophytes (*Cryptomonas sp.*) and dinoflagellates (*Katodinium sp.*, *Peridinium umbonatum*,
418 *Gymnodinium sp.*). These results confirm that mixotrophic strategy and motility are critical for
419 phytoplankton survival under ice (Özkundakci et al., 2016). The autotrophic fraction was
420 mainly composed of small cyanobacteria (*Synechococcus sp.* and *Gomphosphaeria sp.*). This
421 group is known to be cold-tolerant (Jungblut & Vincent, 2017) and has already been observed
422 under ice in oligotrophic lakes (Bullerjahn et al., 2020). In addition, the pool of
423 picocyanobacteria was dominated by phycoerythrin-rich picocyanobacteria (PE_Pcy) during
424 the ice-influenced period. Picocyanobacteria seems to be well adapted to low levels of light and
425 low nutrient concentrations (Callieri et al., 2007; Stomp et al., 2007). Because PE_Pcy use
426 phycoerythrin for harvesting the prevailing green wavelengths, they are well-adapted to poor
427 under-ice light conditions (Jungblut & Vincent, 2017).

428 The overturn period was characterized by a similar phytoplankton biomass but changes in
429 species composition, with more taxa associated with well-mixed systems. Species richness
430 substantially increased, and diversity was at a peak. Changes in phytoplankton community
431 structure have previously been observed after snowmelt as a consequence of meltwater inputs
432 in oligotrophic lakes (Williams et al., 2016), and episodic nutrient enrichments can increase
433 species richness (Zufiaurre et al., 2021). The increased richness and diversity observed during
434 the overturn period was therefore likely the result of nutrient inputs occurring during snowmelt.
435 The proportion of mixotrophs remained the same as in the ice-influenced period and
436 dinoflagellates remained dominant, but small chrysophytes (*Dinobryon divergens*, *Kephyrion*
437 *spirale*) prevailed over cryptophytes during the overturn period. This replacement is not
438 surprising: chrysophytes, especially *Dinobryon*, are known to be obligatory phototrophs

439 (Princiotta et al., 2016) and to form resting stages to withstand adverse environmental
440 conditions (Özkundakci et al., 2016). Changes in light spectral composition have been shown
441 to change dominance patterns between cryptophytes and chrysophytes in shallow North
442 Patagonian lakes (Gerea et al., 2017). Here, in the autotrophic fraction of the phytoplankton
443 assemblage, diatoms (*Cyclotella comensis* and *Fragilaria nanana*) replaced the small
444 cyanobacteria. These two species are widely used as an indicator of physico-chemical changes
445 (Cantonati et al., 2021), especially increased water temperatures in alpine lakes (Catalan, Pla,
446 et al., 2002; Sochuliaková et al., 2018). In addition, the PE:PC picocyanobacteria changed
447 during the overturn, and PC_Pcy became dominant over PE_Pcy. This result clearly indicates
448 a modification of the underwater light spectrum, and consequently the pigment composition of
449 picocyanobacteria (Bastidas Navarro et al., 2009). Our results suggest that the drastic changes
450 in temperature, nutrients, and light availability after snowmelt lie behind the changes in
451 phytoplankton community that we observed.

452 Phytoplankton biomass greatly increased during the late summer period, when the
453 phytoplankton assemblage was almost exclusively composed of less edible, large diatoms
454 (mainly *Fragilaria nanana*). While previous studies report that *Fragilaria nanana* prefers
455 nutrient-enriched waters (Cantonati et al., 2019), this species has also been shown to tolerate
456 very small concentrations of nitrogen (Van Dam et al., 1994). Strong diatom development has
457 already been observed in high-altitude lakes in summer, when thermal stability is higher (Tolotti
458 et al., 2007). It appears that the diatoms in our study were more competitive than the other
459 phytoplankton genera during the late summer period, despite the theoretically successful
460 mixotrophic strategy under limiting nutrients and warmer temperatures (Bhutiani et al., 2009).

461 Overall, we observed a major functional change in phytoplankton assemblages over the three
462 periods. Heterotrophy stood out during the ice-influenced period, with the mixotrophy strategy
463 playing a significant role in the community. Then, mixotrophy was progressively overtaken by

464 autotrophy, becoming negligible during the late summer period next to both the quantity of
465 autotrophic biomass and the proportion of autotrophs in the phytoplankton assemblage.

466 **4.3. Functional shifts at the base of the food web**

467 Bacterial biomass showed the lower values during the ice-influenced period, then progressively
468 increased until the last summer period. Despite the low biomass during the ice-influenced
469 period, the observed hypoxia as well as the high proportion of ammonium in the DIN pool
470 indicate that microbial respiration did occur during this period. Anaerobic metabolism of active
471 psychrophilic bacteria certainly occurred, as it was previously demonstrated in during winter in
472 ice-covered lakes (Bullerjahn et al., 2020; Margesin & Miteva, 2011; Bertilsson et al., 2013),
473 and during the ice-free season in deep high-altitude lakes (Llorens-Marès et al., 2020).

474 Regardless of bacterial respiration, dissolved organic matter properties varied over time and
475 may explain the observed variation in bacterial biomass. The refractory DOM may have
476 insufficiently fueled bacteria during the ice-influenced period, as DOM's overall bioavailability
477 typically declines over time when isolated from fresh inputs (Del Giorgio & Davis, 2003). The
478 increase in bacterial biomass during the overturn period was associated to inputs of terrestrial
479 DOM, which could constitute a valuable source of energy and/or inorganic nutrients for
480 bacteria, stimulating more biomass production than respiration (Guillemette et al., 2016). The
481 bacterial biomass continued to increase until the end of the late summer period, during which
482 the high phytoplankton biomass constituted a highly available C source for bacterioplankton.
483 However, temporal trends of bacterial biomass may also result from bacterial interaction with
484 phytoplankton. The high abundance of large phytoflagellates during the ice-influenced period
485 suggests high predation pressure by mixotrophs during this period. Then predation pressure
486 progressively decreased with the observed change in phytoplankton community composition:

487 some large cryptophytes were replaced by small siliceous chrysophytes during the overturn
488 period. In taxa such as *Dinobryon*, phagotrophy appears to be more a complementary nutritive
489 strategy when light is limiting (Saad et al., 2016), and therefore enhanced light availability
490 during the overturn period may have promoted photosynthesis rather than phagotrophy. Finally,
491 autotrophs largely dominated the phytoplankton community during the late summer period,
492 removing the top-down control over bacteria. Our results confirmed that, together with temporal
493 variation in temperature, oxygen, and nutrient concentrations (Zhou et al., 2020), shifts in DOM
494 properties and phytoplankton community exerted a key role in bacterioplankton regulation.

495 Thus, our result showed that phytoplankton control over bacteria changed over time, from a
496 predominantly top-down control exerted by mixotrophs toward a bottom-up control as source
497 of DOM. By occupying the niche of microheterotrophs and preventing the development of
498 heterotrophic nanoflagellates and ciliates, mixotrophs are known to reduce the number of
499 trophic levels, acting as a bypass of C flux toward the grazing chain (Medina-Sánchez et al.,
500 2004; Ward & Follows, 2016). Indeed, we found low ciliate abundance during the ice-
501 influenced period but higher ciliate abundance during the late summer period. These results
502 also suggest a possibly top-down control of ciliates on heterotrophic nanoflagellates, which in
503 turn allowed an increase in bacterial biomass (Haraguchi et al., 2018).

504 The progressively increase of the $\delta^{13}\text{C}_{\text{POM}}$ confirmed our previous assumptions on shifts
505 occurring at the base of the food web. During the ice-influenced period, $\delta^{13}\text{C}_{\text{POM}}$ ranged
506 between -31.80 ‰ at the bottom and -26.70 ‰ at the surface. These low values may confirm
507 (i) the use of isotopically light DIC from anaerobic respiration for phytoplankton
508 photosynthesis, which might contribute to $\delta^{13}\text{C}_{\text{POM}}$ depletion at the bottom (Cole et al., 2002);
509 (ii) the ingestion of anaerobic bacterial prey by mixotrophs, as anaerobic bacteria usually
510 exhibit further depletion in $\delta^{13}\text{C}$ (Grey, 2016). The increase in $\delta^{13}\text{C}_{\text{POM}}$ during the overturn
511 period could result from multiple processes, like increase inputs of allochthonous DOM (Hou

512 et al., 2013), higher CO₂ uptake rates resulting from greater phytoplankton growth (Gu et al.,
513 2006), or change in phytoplankton taxonomic composition (Golubkov et al., 2020; Trochine et
514 al., 2015). In our study, phytoplankton biomass did not increase during the overturn, but both
515 inputs of allochthonous DOM and change in phytoplankton composition with more efficient
516 photosynthesis occurred. Finally, in late summer, the higher $\delta^{13}\text{C}_{\text{POM}}$ values corroborated the
517 higher CO₂ uptake rates associated with greater autotrophic phytoplankton growth (Gu et al.,
518 2006), although precipitation events at the end of this period may also contribute to higher
519 values of $\delta^{13}\text{C}_{\text{POM}}$. Thus, if $\delta^{13}\text{C}$ values in POM did not allow to determine the part of each
520 process during the different periods, the result confirmed that the origin of the carbon
521 transferred in the planktonic food web varied over time.

522 To conclude, in accordance with our last hypothesis, we observed a temporal shift in
523 phytoplankton – bacterioplankton relationships according to lake functioning patterns (**Figure**
524 **8**). During the ice-influenced period, mixotrophic taxa exerted a strong top-down control over
525 bacteria. Then, phytoplankton control progressively shifted to a predominantly bottom-up
526 control by autotrophs that governed the DOM pool of the lake. Considering our three pre-
527 defined periods thus brings to light differences in the functioning of this high-altitude lake and
528 provides new insights into the mechanisms controlling the phytoplankton community. Our
529 study highlights the need to better assess the trophic processes at work between the planktonic
530 constituents of the food web. Further studies should be conducted to determine the vulnerability
531 of high-altitude lakes to the shortened ice-cover and increased connectivity with their
532 catchments that are predicted.

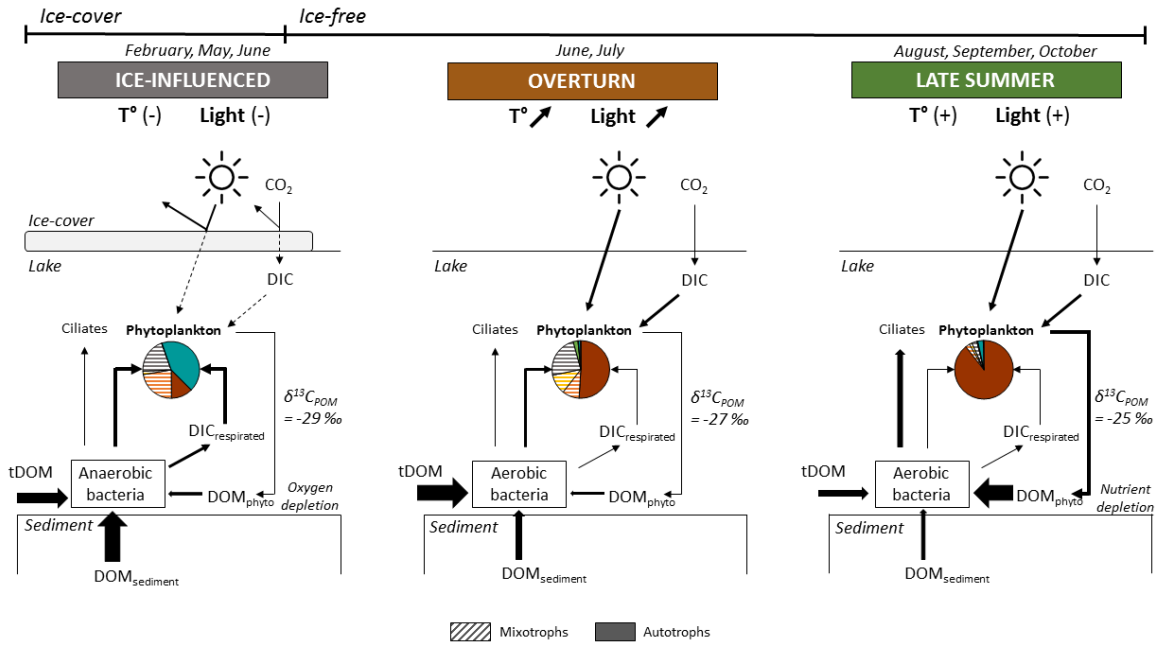


Figure 8: General outline reflecting shifts in phytoplankton control over bacteria in relation to dissolved organic matter properties in the Lake Cordes. tDOM: terrestrial allochthonous DOM; $\text{DOM}_{\text{phyto}}$: autochthonous DOM derived from phytoplankton; DIC: dissolved inorganic carbon; T° : water temperature.

534 ACKNOWLEDGMENTS

535 We are grateful to the members of the French Biodiversity Office, especially René
536 Conraud and Philippe Moullec, for their help in the field. DOC analyses were carried out by
537 the Mediterranean Institute of Oceanography. Chemical data were partly produced through the
538 Biological and Chemical Analysis facilities of IMBE, Marseille. We thank Marjorie Sweetko
539 for improving the English of this manuscript. This work was supported by the French National
540 Program EC2CO (Ecosphère Continentale et Côtière), and forms part of Flavia Dory's PhD
541 thesis, funded by the Ministère de l'Enseignement Supérieur et de la Recherche.

542 **Conflict of interests**

543 The authors declare no conflicts of interest.

544

545 5. REFERENCES

- 546 Aiken, G. (2014). Fluorescence and Dissolved Organic Matter : A Chemist's Perspective. In A.
547 Baker, D. M. Reynolds, J. Lead, P. G. Coble, & R. G. M. Spencer (Éds.), *Aquatic*
548 *Organic Matter Fluorescence* (p. 35-74). Cambridge University Press.
549 <https://doi.org/10.1017/CBO9781139045452.005>
- 550 Anderson, N. J., & Stedmon, C. A. (2007). The effect of evapoconcentration on dissolved
551 organic carbon concentration and quality in lakes of SW Greenland. *Freshwater*
552 *Biology*, 52(2), 280-289. <https://doi.org/10.1111/j.1365-2427.2006.01688.x>
- 553 Bastidas Navarro, M., Balseiro, E., & Modenutti, B. (2014). Bacterial Community Structure in
554 Patagonian Andean Lakes Above and Below Timberline : From Community
555 Composition to Community Function. *Microbial Ecology*, 68(3), 528-541.
556 <https://doi.org/10.1007/s00248-014-0439-9>
- 557 Bastidas Navarro, M., Modenutti, B., Callieri, C., Bertoni, R., & Balseiro, E. (2009). Balance
558 between primary and bacterial production in North Patagonian shallow lakes. *Aquatic*
559 *Ecology*, 43(4), 867-878. <https://doi.org/10.1007/s10452-008-9220-9>
- 560 Bergström, A.-K. (2009). Seasonal dynamics of bacteria and mixotrophic flagellates as related
561 to input of allochthonous dissolved organic carbon. *SIL Proceedings, 1922-2010*, 30(6),
562 923-928. <https://doi.org/10.1080/03680770.2009.11902273>
- 563 Bertilsson, S., Burgin, A., Carey, C. C., Fey, S. B., Grossart, H.-P., Grubisic, L. M., Jones, I.
564 D., Kirillin, G., Lennon, J. T., Shade, A., & Smyth, R. L. (2013). The under-ice
565 microbiome of seasonally frozen lakes. *Limnology and Oceanography*, 58(6), 1998-
566 2012. <https://doi.org/10.4319/lo.2013.58.6.1998>

567 Bhutiani, R., Khanna, D. R., & Chandra, K. S. (2009). Light-limited population dynamics of
568 phytoplankton : Modeling light and depth effects. *The Environmentalist*, 29(1), 93-105.
569 <https://doi-org.lama.univ-amu.fr/10.1007/s10669-008-9184-2>

570 Bullerjahn, G. S., McKay, R. M. L., Bernat, G., Prasil, O., Voros, L., Palfy, K., Tugyi, N., &
571 Somogyi, B. (2020). Community dynamics and function of algae and bacteria during
572 winter in central European great lakes. *Journal of Great Lakes Research*, 46(4), 732-
573 740. <https://doi.org/10.1016/j.jglr.2019.07.002>

574 Callieri, C., Modenutti, B., Queimaliños, C., Bertoni, R., & Balseiro, E. (2007). Production and
575 biomass of picophytoplankton and larger autotrophs in Andean ultraoligotrophic lakes :
576 Differences in light harvesting efficiency in deep layers. *Aquatic Ecology*, 41(4), 511-
577 523. <https://doi.org/10.1007/s10452-007-9125-z>

578 Cantonati, M., Angeli, N., & Lange-Bertalot, H. (2019). Three new *Fragilaria* species
579 (Bacillariophyta) from low-conductivity mountain freshwaters (Alps and Apennines).
580 *Phytotaxa*, 404(6), 261-274-261-274. <https://doi.org/10.11646/phytotaxa.404.6.5>

581 Cantonati, M., Zorza, R., Bertoli, M., Pastorino, P., Salvi, G., Platania, G., Prearo, M., & Pizzul,
582 E. (2021). Recent and subfossil diatom assemblages as indicators of environmental
583 change (including fish introduction) in a high-mountain lake. *Ecological Indicators*,
584 125, 107603. <https://doi.org/10.1016/j.ecolind.2021.107603>

585 Catalan, J., Pla, S., Rieradevall, M., Felip, M., Ventura, M., Buchaca, T., Camarero, L.,
586 Brancelj, A., Appleby, P. G., Lami, A., Grytnes, J. A., Agustí-Panareda, A., &
587 Thompson, R. (2002). Lake Redó ecosystem response to an increasing warming the
588 Pyrenees during the twentieth century. *Journal of Paleolimnology*, 28(1), 129-145.
589 <https://doi.org/10.1023/A:1020380104031>

590 Catalan, J., Ventura, M., Brancelj, A., Granados, I., Thies, H., Nickus, U., Korhola, A., Lotter,
591 A. F., Barbieri, A., & Stuchlik, E. (2002). Seasonal ecosystem variability in remote

592 mountain lakes : Implications for detecting climatic signals in sediment records. *Journal*
593 *of Paleolimnology*, 28(1), 25-46. <https://doi.org/10.1023/A:1020315817235>

594 Catalán, N., Obrador, B., Felip, M., & Pretus, J. L. (2013). Higher reactivity of allochthonous
595 vs. Autochthonous DOC sources in a shallow lake. *Aquatic sciences*, 75(4), 581-593.
596 <https://doi.org/10.1007/s00027-013-0302-y>

597 Chen, W., Westerhoff, P., Leenheer, J. A., & Booksh, K. (2003). Fluorescence
598 Excitation–Emission Matrix Regional Integration to Quantify Spectra for Dissolved
599 Organic Matter. *Environmental Science & Technology*, 37(24), 5701-5710.
600 <https://doi.org/10.1021/es034354c>

601 Cole, J. J., Carpenter, S. R., Kitchell, J. F., & Pace, M. L. (2002). Pathways of organic carbon
602 utilization in small lakes : Results from a whole-lake ¹³C addition and coupled model.
603 *Limnology and Oceanography*, 47(6), 1664-1675.
604 <https://doi.org/10.4319/lo.2002.47.6.1664>

605 Cory, R. M., & McKnight, D. M. (2005). Fluorescence Spectroscopy Reveals Ubiquitous
606 Presence of Oxidized and Reduced Quinones in Dissolved Organic Matter.
607 *Environmental Science & Technology*, 39(21), 8142-8149.
608 <https://doi.org/10.1021/es0506962>

609 Creed, I. F., Bergström, A.-K., Trick, C. G., Grimm, N. B., Hessen, D. O., Karlsson, J., Kidd,
610 K. A., Kritzberg, E., McKnight, D. M., Freeman, E. C., Senar, O. E., Andersson, A.,
611 Ask, J., Berggren, M., Cherif, M., Giesler, R., Hotchkiss, E. R., Kortelainen, P., Palta,
612 M. M., ... Weyhenmeyer, G. A. (2018). Global change-driven effects on dissolved
613 organic matter composition : Implications for food webs of northern lakes. *Global*
614 *Change Biology*, 24(8), 3692-3714. <https://doi.org/10.1111/gcb.14129>

615 Del Giorgio, P. A., & Davis, J. (2003). Patterns in Dissolved Organic Matter Lability and
616 Consumption across Aquatic Ecosystems. In S. E. G. Findlay & R. L. Sinsabaugh

617 (Éds.), *Aquatic Ecosystems* (p. 399-424). Academic Press.
618 <https://doi.org/10.1016/B978-012256371-3/50018-4>

619 Dory, F., Cavalli, L., Franquet, E., Claeys-Bruno, M., Misson, B., Tatoni, T., & Bertrand, C.
620 (2021a). Microbial consortia in an ice-covered high-altitude lake impacted by additions
621 of dissolved organic carbon and nutrients. *Freshwater Biology*, 66(8), 1648-1662.
622 <https://doi.org/10.1111/fwb.13781>

623 Dory, F., Cavalli, L., Franquet, E., Claeys-Bruno, M., Misson, B., Tatoni, T., & Bertrand, C.
624 (2021b). *Summer dynamics drive the microbial response to DOC additions in a high*
625 *altitude lake.*

626 Du, Y., Zhang, Y., Chen, F., Chang, Y., & Liu, Z. (2016). Photochemical reactivities of
627 dissolved organic matter (DOM) in a sub-alpine lake revealed by EEM-PARAFAC : An
628 insight into the fate of allochthonous DOM in alpine lakes affected by climate change.
629 *Science of The Total Environment*, 568, 216-225.
630 <https://doi.org/10.1016/j.scitotenv.2016.06.036>

631 Felip, M., Wille, A., Sattler, B., & Psenner, R. (2002). Microbial communities in the winter
632 cover and the water column of an alpine lake : System connectivity and uncoupling.
633 *Aquatic Microbial Ecology*, 29, 123-134. <https://doi.org/10.3354/ame029123>

634 Gabor, R. S., Baker, A., McKnight, D. M., & Miller, M. P. (2014). Fluorescence indices and
635 their interpretation. *Aquatic organic matter fluorescence*, 303.

636 Gereá, M., Pérez, G. L., Unrein, F., Soto Cárdenas, C., Morris, D., & Queimaliños, C. (2017).
637 CDOM and the underwater light climate in two shallow North Patagonian lakes :
638 Evaluating the effects on nano and microphytoplankton community structure. *Aquatic*
639 *Sciences*, 79(2), 231-248. <https://doi.org/10.1007/s00027-016-0493-0>

640 Golubkov, M. S., Nikulina, V. N., Tiunov, A. V., & Golubkov, S. M. (2020). Stable C and N
641 Isotope Composition of Suspended Particulate Organic Matter in the Neva Estuary : The

642 Role of Abiotic Factors, Productivity, and Phytoplankton Taxonomic Composition.
643 *Journal of Marine Science and Engineering*, 8(12), 959.
644 <https://doi.org/10.3390/jmse8120959>

645 Grey, J. (2016). The Incredible Lightness of Being Methane-Fuelled : Stable Isotopes Reveal
646 Alternative Energy Pathways in Aquatic Ecosystems and Beyond. *Frontiers in Ecology*
647 *and Evolution*, 4, 8. <https://doi.org/10.3389/fevo.2016.00008>

648 Gu, B., Chapman, A. D., & Schelske, C. L. (2006). Factors controlling seasonal variations in
649 stable isotope composition of particulate organic matter in a softwater eutrophic lake.
650 *Limnology and Oceanography*, 51(6), 2837-2848.
651 <https://doi.org/10.4319/lo.2006.51.6.2837>

652 Guillemette, F., McCallister, S. L., & del Giorgio, P. A. (2016). Selective consumption and
653 metabolic allocation of terrestrial and algal carbon determine allochthony in lake
654 bacteria. *The ISME Journal*, 10(6), 1373-1382. <https://doi.org/10.1038/ismej.2015.215>

655 Haraguchi, L., Jakobsen, H. H., Lundholm, N., & Carstensen, J. (2018). Phytoplankton
656 Community Dynamic : A Driver for Ciliate Trophic Strategies. *Frontiers in Marine*
657 *Science*, 5. <https://doi.org/10.3389/fmars.2018.00272>

658 Harsch, M. A., Hulme, P. E., McGlone, M. S., & Duncan, R. P. (2009). Are treelines advancing?
659 A global meta-analysis of treeline response to climate warming. *Ecology Letters*,
660 12(10), 1040-1049. <https://doi.org/10.1111/j.1461-0248.2009.01355.x>

661 Hou, W., Gu, B., Lin, Q., Gu, J., & Han, B.-P. (2013). Stable isotope composition of suspended
662 particulate organic matter in twenty reservoirs from Guangdong, southern China :
663 Implications for pelagic carbon and nitrogen cycling. *Water Research*, 47(11), 3610-
664 3623. <https://doi.org/10.1016/j.watres.2013.04.014>

665 Jacquemin, C., Bertrand, C., Franquet, E., Mounier, S., Misson, B., Oursel, B., & Cavalli, L.
666 (2019). Effects of catchment area and nutrient deposition regime on phytoplankton

667 functionality in alpine lakes. *Science of The Total Environment*, 674, 114-127.
668 <https://doi.org/10.1016/j.scitotenv.2019.04.117>

669 Jacquemin, C., Bertrand, C., Oursel, B., Thorel, M., Franquet, E., & Cavalli, L. (2018). Growth
670 rate of alpine phytoplankton assemblages from contrasting watersheds and N-deposition
671 regimes exposed to nitrogen and phosphorus enrichments. *Freshwater Biology*, 63(10),
672 1326-1339. <https://doi.org/10.1111/fwb.13160>

673 Jansson, M., Bergström, A.-K., Blomqvist, P., & Drakare, S. (2000). Allochthonous Organic
674 Carbon and Phytoplankton/Bacterioplankton Production Relationships in Lakes.
675 *Ecology*, 81(11), 3250-3255. [https://doi.org/10.1890/0012-](https://doi.org/10.1890/0012-9658(2000)081[3250:AOCAPB]2.0.CO;2)
676 [9658\(2000\)081\[3250:AOCAPB\]2.0.CO;2](https://doi.org/10.1890/0012-9658(2000)081[3250:AOCAPB]2.0.CO;2)

677 Jungblut, A. D., & Vincent, W. F. (2017). Cyanobacteria in Polar and Alpine Ecosystems. In
678 R. Margesin (Éd.), *Psychrophiles : From Biodiversity to Biotechnology* (p. 181-206).
679 Springer International Publishing. https://doi.org/10.1007/978-3-319-57057-0_9

680 Karlsson, J., Ask, J., & Jansson, M. (2008). Winter respiration of allochthonous and
681 autochthonous organic carbon in a subarctic clear-water lake. *Limnology and*
682 *Oceanography*, 53(3), 948-954. <https://doi.org/10.4319/lo.2008.53.3.0948>

683 Kruk, C., Huszar, V. L. M., Peeters, E. T. H. M., Bonilla, S., Costa, L., LüRling, M., Reynolds,
684 C. S., & Scheffer, M. (2010). A morphological classification capturing functional
685 variation in phytoplankton. *Freshwater Biology*, 55(3), 614-627.
686 <https://doi.org/10.1111/j.1365-2427.2009.02298.x>

687 Kuefner, W., Hofmann, A. M., Geist, J., Dubois, N., & Raeder, U. (2021). Algal Community
688 Change in Mountain Lakes of the Alps Reveals Effects of Climate Warming and
689 Shifting Treelines. *Journal of Phycology*, 57(4), 1266-1283.
690 <https://doi.org/10.1111/jpy.13163>

691 Linacre, L., Lara-Lara, R., Camacho-Ibar, V., Herguera, J. C., Bazán-Guzmán, C., & Ferreira-
692 Bartrina, V. (2015). Distribution pattern of picoplankton carbon biomass linked to
693 mesoscale dynamics in the southern gulf of Mexico during winter conditions. *Deep Sea*
694 *Research Part I: Oceanographic Research Papers*, 106, 55-67.
695 <https://doi.org/10.1016/j.dsr.2015.09.009>

696 Llorens-Marès, T., Catalan, J., & Casamayor, E. O. (2020). Taxonomy and functional
697 interactions in upper and bottom waters of an oligotrophic high-mountain deep lake
698 (Redon, Pyrenees) unveiled by microbial metagenomics. *Science of The Total*
699 *Environment*, 707, 135929. <https://doi.org/10.1016/j.scitotenv.2019.135929>

700 McKnight, D. M., Smith, R. L., Bradbury, J. P., Baron, J. S., & Spaulding, S. (1990).
701 Phytoplankton Dynamics in Three Rocky Mountain Lakes, Colorado, U.S.A. *Arctic and*
702 *Alpine Research*, 22(3), 264-274. <https://doi.org/10.1080/00040851.1990.12002790>

703 Medina-Sánchez, J. M., Villar-Argaiz, M., & Carrillo, P. (2004). Neither with nor without you :
704 A complex algal control on bacterioplankton in a high mountain lake. *Limnology and*
705 *Oceanography*, 49(5), 1722-1733. <https://doi.org/10.4319/lo.2004.49.5.1722>

706 Miller, M. P., McKnight, D. M., Chapra, S. C., & Williams, M. W. (2009). A model of
707 degradation and production of three pools of dissolved organic matter in an alpine lake.
708 *Limnology and Oceanography*, 54(6), 2213-2227.
709 <https://doi.org/10.4319/lo.2009.54.6.2213>

710 Mitra, A., Flynn, K. J., Tillmann, U., Raven, J. A., Caron, D., Stoecker, D. K., Not, F., Hansen,
711 P. J., Hallegraeff, G., Sanders, R., Wilken, S., McManus, G., Johnson, M., Pitta, P.,
712 Våge, S., Berge, T., Calbet, A., Thingstad, F., Jeong, H. J., ... Lundgren, V. (2016).
713 Defining Planktonic Protist Functional Groups on Mechanisms for Energy and Nutrient
714 Acquisition : Incorporation of Diverse Mixotrophic Strategies. *Protist*, 167(2), 106-
715 120. <https://doi.org/10.1016/j.protis.2016.01.003>

716 Moser, K. A., Baron, J. S., Brahney, J., Oleksy, I. A., Saros, J. E., Hundey, E. J., Sadro, S. A.,
717 Kopáček, J., Sommaruga, R., Kainz, M. J., Strecker, A. L., Chandra, S., Walters, D. M.,
718 Preston, D. L., Michelutti, N., Lepori, F., Spaulding, S. A., Christianson, K. R., Melack,
719 J. M., & Smol, J. P. (2019). Mountain lakes : Eyes on global environmental change.
720 *Global and Planetary Change*, 178, 77-95.
721 <https://doi.org/10.1016/j.gloplacha.2019.04.001>

722 Murphy, K. R., Stedmon, C. A., Waite, T. D., & Ruiz, G. M. (2008). Distinguishing between
723 terrestrial and autochthonous organic matter sources in marine environments using
724 fluorescence spectroscopy. *Marine Chemistry*, 108(1), 40-58.
725 <https://doi.org/10.1016/j.marchem.2007.10.003>

726 Ohno, T. (2002). Fluorescence Inner-Filtering Correction for Determining the Humification
727 Index of Dissolved Organic Matter. *Environmental Science & Technology*, 36(4), 742-
728 746. <https://doi.org/10.1021/es0155276>

729 Oleksy, I. A., Beck, W. S., Lammers, R. W., Steger, C. E., Wilson, C., Christianson, K.,
730 Vincent, K., Johnson, G., Johnson, P. T. J., & Baron, J. S. (2020). The role of warm,
731 dry summers and variation in snowpack on phytoplankton dynamics in mountain lakes.
732 *Ecology*, 101(10), e03132. <https://doi.org/10.1002/ecy.3132>

733 Olson, M. H., Fischer, J. M., & Hayashi, M. (2021). Temporal dynamics of dissolved organic
734 matter (DOM) in mountain lakes : The role of catchment characteristics. *Canadian*
735 *Journal of Fisheries and Aquatic Sciences*. <https://doi.org/10.1139/cjfas-2020-0421>

736 Özkundakci, D., Gsell, A. S., Hintze, T., Täuscher, H., & Adrian, R. (2016). Winter severity
737 determines functional trait composition of phytoplankton in seasonally ice-covered
738 lakes. *Global Change Biology*, 22(1), 284-298. <https://doi.org/10.1111/gcb.13085>

739 Padisák, J., Crossetti, L. O., & Naselli-Flores, L. (2009). Use and misuse in the application of
740 the phytoplankton functional classification: A critical review with updates.
741 *Hydrobiologia*, 621(1), 1-19. <https://doi.org/10.1007/s10750-008-9645-0>

742 Perga, M.-E., Bruel, R., Rodriguez, L., Guénand, Y., & Bouffard, D. (2018). Storm impacts on
743 alpine lakes: Antecedent weather conditions matter more than the event intensity.
744 *Global Change Biology*, 24(10), 5004-5016. <https://doi.org/10.1111/gcb.14384>

745 Princiotta, S. D., Smith, B. T., & Sanders, R. W. (2016). Temperature-dependent phagotrophy
746 and phototrophy in a mixotrophic chrysophyte. *Journal of Phycology*, 52(3), 432-440.
747 <https://doi.org/10.1111/jpy.12405>

748 Pulido-Villena, E., Reche, I., & Morales-Baquero, R. (2008). Evidence of an atmospheric
749 forcing on bacterioplankton and phytoplankton dynamics in a high mountain lake.
750 *Aquatic Sciences*, 70(1), 1-9. <https://doi.org/10.1007/s00027-007-0944-8>

751 Queimaliños, C., Reissig, M., Pérez, G. L., Soto Cárdenas, C., Gereá, M., Garcia, P. E., García,
752 D., & Diéguez, M. C. (2019). Linking landscape heterogeneity with lake dissolved
753 organic matter properties assessed through absorbance and fluorescence spectroscopy:
754 Spatial and seasonal patterns in temperate lakes of Southern Andes (Patagonia,
755 Argentina). *Science of The Total Environment*, 686, 223-235.
756 <https://doi.org/10.1016/j.scitotenv.2019.05.396>

757 Redon, R. (2018). *Progmeef*. <https://woms18.univ-tln.fr/progmeef/> (2018)

758 Reynolds, C. S., Huszar, V., Kruk, C., Naselli-Flores, L., & Melo, S. (2002). Towards a
759 functional classification of the freshwater phytoplankton. *Journal of Plankton Research*,
760 24(5), 417-428. <https://doi.org/10.1093/plankt/24.5.417>

761 Rose, K. C., Williamson, C. E., Kissman, C. E. H., & Saros, J. E. (2015). Does allochthony in
762 lakes change across an elevation gradient? *Ecology*, *96*(12), 3281-3291.
763 <https://doi.org/10.1890/14-1558.1>

764 Rue, G. P., Darling, J. P., Graham, E., Tfaily, M. M., & McKnight, D. M. (2020). Dynamic
765 changes in dissolved organic matter composition in a Mountain Lake under ice cover
766 and relationships to changes in nutrient cycling and phytoplankton community
767 composition. *Aquatic Sciences*, *82*(1), 15. <https://doi.org/10.1007/s00027-019-0687-3>

768 Saad, J. F., Unrein, F., Tribelli, P. M., López, N., & Izaguirre, I. (2016). Influence of lake
769 trophic conditions on the dominant mixotrophic algal assemblages. *Journal of Plankton
770 Research*, *38*(4), 818-829. <https://doi.org/10.1093/plankt/fbw029>

771 Sadro, S., & Melack, J. M. (2012). The effect of an extreme rain event on the biogeochemistry
772 and ecosystem metabolism of an oligotrophic high-elevation lake. *Arctic, Antarctic, and
773 Alpine Research*, *44*(2), 222-231. <https://doi.org/10.1657/1938-4246-44.2.222>

774 Sadro, S., Melack, J. M., & MacIntyre, S. (2011). Spatial and Temporal Variability in the
775 Ecosystem Metabolism of a High-elevation Lake : Integrating Benthic and Pelagic
776 Habitats. *Ecosystems*, *14*(7), 1123-1140. <https://doi.org/10.1007/s10021-011-9471-5>

777 Sochuliaková, L., Sienkiewicz, E., Hamerlík, L., Svitok, M., Fidlerová, D., & Bitušík, P.
778 (2018). Reconstructing the Trophic History of an Alpine Lake (High Tatra Mts.) Using
779 Subfossil Diatoms : Disentangling the Effects of Climate and Human Influence. *Water,
780 Air, & Soil Pollution*, *229*(9), 289. <https://doi.org/10.1007/s11270-018-3940-9>

781 Sommaruga, R., & Augustin, G. (2006). Seasonality in UV transparency of an alpine lake is
782 associated to changes in phytoplankton biomass. *Aquatic Sciences*, *68*(2), 129-141.
783 <https://doi.org/10.1007/s00027-006-0836-3>

784 Stomp, M., Huisman, J., Vörös, L., Pick, F. R., Laamanen, M., Haverkamp, T., & Stal, L. J.
785 (2007). Colourful coexistence of red and green picocyanobacteria in lakes and seas.
786 *Ecology Letters*, 10(4), 290-298. <https://doi.org/10.1111/j.1461-0248.2007.01026.x>

787 Tiberti, R., Metta, S., Austoni, M., Callieri, C., Giuseppe, M., Aldo, M., Rogora, M., Tartari,
788 G. A., Hardenberg, J. V., & Provenzale, A. (2013). Ecological dynamics of two remote
789 alpine lakes during ice-free season. *Journal of Limnology*, 72(3), e33-e33.
790 <https://doi.org/10.4081/jlimnol.2013.e33>

791 Tolotti, M., Corradini, F., Boscaini, A., & Calliari, D. (2007). Weather-driven ecology of
792 planktonic diatoms in Lake Tovel (Trentino, Italy). *Hydrobiologia*, 578(1), 147-156.
793 <https://doi.org/10.1007/s10750-006-0441-4>

794 Trochine, C., Díaz Villanueva, V., Bastidas Navarro, M., Balseiro, E., & Modenutti, B. (2015).
795 The abundance of mixotrophic algae drives the carbon isotope composition of the
796 copepod *Boeckella gracilipes* in shallow Patagonian lakes. *Journal of Plankton*
797 *Research*, 37(2), 441-451. <https://doi.org/10.1093/plankt/fbv005>

798 Utermöhl, H. (1958). Methods of collecting plankton for various purposes are discussed. *SIL*
799 *Communications*, 1953-1996, 9(1), 1-38.
800 <https://doi.org/10.1080/05384680.1958.11904091>

801 Van Dam, H., Mertens, A., & Sinkeldam, J. (1994). A coded checklist and ecological indicator
802 values of freshwater diatoms from The Netherlands. *Netherland Journal of Aquatic*
803 *Ecology*, 28(1), 117-133. <https://doi.org/10.1007/BF02334251>

804 Ward, B. A., & Follows, M. J. (2016). Marine mixotrophy increases trophic transfer efficiency,
805 mean organism size, and vertical carbon flux. *Proceedings of the National Academy of*
806 *Sciences*, 113(11), 2958-2963. <https://doi.org/10.1073/pnas.1517118113>

807 Wetzel, R. G., & Likens, G. E. (2000). Composition and Biomass of Phytoplankton. In R. G.
808 Wetzel & G. E. Likens (Éds.), *Limnological Analyses* (Springer, p. 147-174).
809 https://doi.org/10.1007/978-1-4757-3250-4_10

810 Williams, J. J., Nurse, A., Saros, J. E., Riedel, J., & Beutel, M. (2016). Effects of glaciers on
811 nutrient concentrations and phytoplankton in lakes within the Northern Cascades
812 Mountains (USA). *Biogeochemistry*, *131*(3), 373-385. [https://doi.org/10.1007/s10533-](https://doi.org/10.1007/s10533-016-0264-y)
813 [016-0264-y](https://doi.org/10.1007/s10533-016-0264-y)

814 Zhou, S., Sun, Y., Yu, M., Shi, Z., Zhang, H., Peng, R., Li, Z., Cui, J., & Luo, X. (2020). Linking
815 Shifts in Bacterial Community Composition and Function with Changes in the
816 Dissolved Organic Matter Pool in Ice-Covered Baiyangdian Lake, Northern China.
817 *Microorganisms*, *8*(6), 883. <https://doi.org/10.3390/microorganisms8060883>

818 Zufiaurre, A., Felip, M., Giménez-Grau, P., Pla-Rabès, S., Camarero, L., & Catalan, J. (2021).
819 Episodic nutrient enrichments stabilise protist coexistence in planktonic oligotrophic
820 conditions. *Journal of Ecology*, *109*(4), 1717-1729. [https://doi.org/10.1111/1365-](https://doi.org/10.1111/1365-2745.13591)
821 [2745.13591](https://doi.org/10.1111/1365-2745.13591)

822